

Rate-Controlling Events for Radical Exit in Electrosterically Stabilized Emulsion Polymerization Systems

Stuart C. Thickett and Robert G. Gilbert*

Key Centre for Polymer Colloids, School of Chemistry F11, Sydney University, NSW 2006, Australia

Received October 13, 2005; Revised Manuscript Received January 29, 2006

ABSTRACT: The mechanism controlling radical loss by exit (desorption) in electrosterically stabilized emulsion polymerization particles was obtained from kinetic studies. Using RAFT-controlled radical polymerization techniques, polystyrene particles stabilized with differing lengths of poly(acrylic acid) chains bound to the surface were synthesized, with the hydrophilic block of low polydispersity, and of various degrees of polymerization. After removal of the RAFT agent, these latexes were used in seeded emulsion polymerization experiments with styrene, with the radical loss kinetics studied through the use of γ -radiolysis dilatometry. The size of the particles is such that they follow “zero–one” kinetics, so the sole rate-determining step for radical loss is by exit. The rate coefficient for exit (k) of these latexes was obtained directly from the non-steady-state relaxation period. A significant decrease in k occurs (by a factor of 10) relative to ionically stabilized latexes of corresponding size, even for particles with very small hydrophilic layers. The value of k was smaller for latexes with greater length of the hydrophilic block, consistent with the hypothesis that exit in electrosterically stabilized systems is bound by a restricted diffusion through the hydrophilic polymeric layer on the surface. Modification of the Smoluchowski treatment for diffusion-controlled rate coefficients to allow for diffusion through two different regions provides an expression for the rate coefficient of radical desorption out of a particle in these systems; semiquantitative agreement with experiment was obtained.

Introduction

Emulsion polymerization systems are commonly made on an industrial scale through the copolymerization of a hydrophobic monomer (butyl acrylate, styrene, etc.) with a hydrophilic carboxylic monomer (such as acrylic acid), to provide enhanced colloidal stability. The water-soluble monomer preferentially polymerizes in the aqueous phase and then enters the particle when it has a sufficiently hydrophobic component, forming chains that are anchored (grafted) to the particle surface, giving the particle both steric and electrostatic stabilization (if the monomer can be ionized). In addition, stabilization through the addition of steric stabilizers is common; such added steric stabilizers have a water-soluble polymeric component but are not grafted to the particle. For all (electro)steric-stabilized particles, the water-soluble polymeric component forms a “hairy layer” around the particle.

As industrial formulations often employ electrosteric stabilization, it is desirable to understand quantitatively the effect these water-soluble chains have on the polymerization kinetics in order to better control latex synthesis and final properties. *Ab initio* experiments using block polyelectrolytes as surfactants in emulsion polymerization systems demonstrated that the combination of charge of the entering radical as well as the charge of the hydrophilic block had a major impact on the overall polymerization rate, suggesting diffusion was a rate-determining step.¹ In the same work an increase in “surfactant” concentration led to a decrease in the overall rate; this is the exact opposite to what the early work of Smith and Ewart² proposed, clearly indicating that electrosteric systems behave differently to those stabilized by ionic surfactants. The complications of the particle formation mechanism, however, make determination of rate coefficients near impossible from this work.

To avoid the kinetic complications associated with particle formation, seeded dilatometric experiments have become established as the method of choice in order to determine the kinetics of particle growth.³ If intraparticle termination is not rate determining (i.e., if an entering radical will instantaneously terminate a growing radical already inside the particle, defining a “zero–one” system), then the rate coefficients for entry and exit can be determined directly from appropriate rate data. For the emulsion polymerization of styrene at 50 °C, it has been confirmed experimentally⁴ and theoretically⁵ that this condition applies for small particles (<100 nm diameter).

The methodology used here to obtain the exit rate coefficient requires that the system be zero–one, which enables this rate coefficient to be deduced from the data with essentially no model-based assumptions. However, the mechanistic inferences deduced from the rate coefficients so obtained (e.g., for the dependence of the rate coefficient for radical desorption on the degree of polymerization of the hairs) should be applicable to any emulsion polymerization system, zero–one or otherwise.

For ionically stabilized poly(styrene) latexes, experimental entry and exit rate coefficient values, obtained with the same methodology applied here for electrosterically stabilized particles, have shown very good agreement with currently accepted theoretical models for a wide range of systems.^{6–9}

The aim of this work is to compare the kinetics of electrosterically stabilized latex particles to the better understood ionically stabilized system, to quantify the impact of electrosteric stabilization. Only limited work has been previously done on this subject, with the most recent work of Vorwerk and Gilbert¹⁰ revealing ambiguous results with respect to the entry and exit rate coefficients. Using a poly(styrene) seed latex that was then polymerized further in the presence of acrylic acid and styrene to create an electrosterically stabilized latex, it was shown that both the entry (ρ) and exit (k) rate coefficient in these systems were reduced (this included corrections to earlier work by Coen et al.¹¹). A significant pH dependence was also seen in the work

* Corresponding author. Fax: +61–2–9351 8651. Telephone: +61 2 9351 3366. E-mail: gilbert@chem.usyd.edu.au.

of Vorwerg, with significant secondary nucleation seen at neutral pH values and a significant decrease in ρ and k , demonstrating the significance of the nature of the hairy layer and the effect that restricting the ability for an entering (or exiting) radical can have on polymerization kinetics. The major problem in extracting quantitative trends from this type of work is that by building a hairy layer via conventional free radical polymerization, the molecular weight distribution (MWD) of the hydrophilic blocks on the particle surface is very broad; moreover, measuring the width of this layer is extremely difficult.¹² This makes any inferences regarding the polymerization rate as a function of layer size impossible.

Recent developments in controlled radical polymerization in emulsion from Ferguson et al.¹³ have since enabled the synthesis of latex particles with a hairy layer of well-defined width (i.e., narrow molecular weight distribution). Using an amphipathic RAFT (reversible addition fragmentation chain transfer) agent dissolved in water, polymerization of a hydrophilic monomer such as acrylic acid (AA) takes place, with the AA:RAFT molar ratio dictating the average length of hydrophilic block. As these chains are capped with the RAFT end group at the conclusion of the reaction, the chains are still active but lie dormant and can be further polymerized with another monomer.¹⁴ Using a hydrophobic monomer such as butyl acrylate or styrene under starved-feed conditions (to prevent droplet nucleation^{13,15}), further polymerization takes place in the aqueous phase until the hydrophobic block reaches a critical length such that self-assembly of the polymer chains takes place, leading to particle formation. This "RAFT-controlled self-assembly" technique allows, for the first time, the synthesis of electrosterically stabilized polymer colloids where the stabilizing unit can be characterized and is relatively monodisperse, and it is hence ideal for inferring mechanistic understanding from seeded kinetic studies.

The area of polymerization kinetics investigated in this work is the kinetics of radical exit in particles with stabilizing units of different length. Direct measurement of k (the exit rate coefficient) has been achievable through the use of γ -relaxation dilatometry. γ -Radiation can be used to initiate polymerization in an emulsion system¹⁶ through the formation of $\cdot\text{OH}$ and $\cdot\text{H}$ radicals in the aqueous phase. Unlike the use of chemical initiators, the initiating radical flux can be switched off by removing the polymerization vessel from the radiation source. This leads to the polymerization rate decreasing as a function of time, indicating the loss of active radicals at the polymerization locus—directly attributable to radical exit if the particles are sufficiently small (because exited radicals may reenter a particle which contains a growing chain, with termination then ensuing). From this, a direct determination of k can be made by fitting experimental data to the appropriate rate equation.³ Knowledge of k further allows us to determine the rate of radical entry unambiguously in a corresponding system with chemical initiation, making elucidation of polymerization mechanisms possible. With detailed theoretical mechanisms for radical exit well established,⁵ this work will allow us to determine whether radical exit in electrosterically stabilized systems is fundamentally different to what is predicted, with the aim of being able to rationalize any mechanistic differences.

Theory

Emulsion Polymerization Rate Equations. The rate in an emulsion polymerization is given by

$$\frac{dx}{dt} = \frac{k_p[M]_p N_p \bar{n}}{n_M^0 N_{Av}} \quad (1)$$

where x = fractional conversion, k_p = propagation rate coefficient, $[M]_p$ = monomer concentration inside the particles, n_M^0 = initial monomer concentration per unit volume of aqueous phase, N_p = particle number per unit volume of aqueous phase, N_{Av} = the Avogadro constant, and \bar{n} = average number of radicals per particle. Equation 1 is used to obtain \bar{n} from experimental rate data (for systems where no secondary nucleation takes place). For styrene at 50 °C, it has been shown that monomeric styryl radicals formed by transfer exit a particle then reenter another particle without reescaping (known as limit 2a).³ This leads to the kinetic equation

$$\frac{d\bar{n}}{dt} = \rho(1 - 2\bar{n}) - 2k\bar{n}^2 \quad (2)$$

where ρ is the pseudo-first-order rate coefficient for the number of entry events per radical per unit time, and k is the exit rate coefficient of radicals per particle. The entry rate coefficient is normally described as the sum of the initiator-derived entry events as well as the spontaneous or "thermal" entry component. During γ -relaxation experiments the only contribution is from spontaneous entry. Fitting eq 2 to experimental data in the relaxation period yields k and ρ_{spont} . What is important about this zero-one treatment is that these two rate coefficients are deduced in an unambiguous way from experimental data, data which have been shown to contain no more than two independent pieces of information: for example, the shape of the relaxation rate can be reproduced within experimental uncertainty by just two parameters, the long-time slope and intercept of $x(t)$.^{17,18} Thus, this methodology will yield unique values of two rate coefficients from data which contain only two independent pieces of information.

Currently Accepted Exit Model. This model is essentially that developed by Nomura, Hansen and Ugelstad.^{6–9} As monomeric styryl radicals formed by transfer reactions to monomer (with rate coefficient k_{tr}) are the only species that can possibly diffuse out of a particle into the aqueous phase due to moderate water solubility, the rate of radical exit is controlled by the fate of this species. Assuming that this radical can only diffuse through the water phase (with diffusion coefficient D_w) or propagate (with rate coefficient k_p), the rate coefficient for radical exit is given by⁷

$$k = \frac{k_{dM}k_{tr}}{k_p} \quad (3)$$

where

$$k_{dM} = \frac{3D_w}{r_s^2} \frac{[M]_w}{[M]_p} \quad (4)$$

where r_s is the swollen radius of the particle and $[M]_w$ is the monomer concentration in the aqueous phase. This model provides good predictive accuracy for ionically stabilized styrene emulsion polymerization systems, and it will be tested in this work.

Experimental Section

Reagents. Acrylic acid (AA) (Sumika) was purified by vacuum distillation to remove dimeric structures and polymerization inhibitors. Styrene (Sigma Aldrich) was purified by passing the monomer

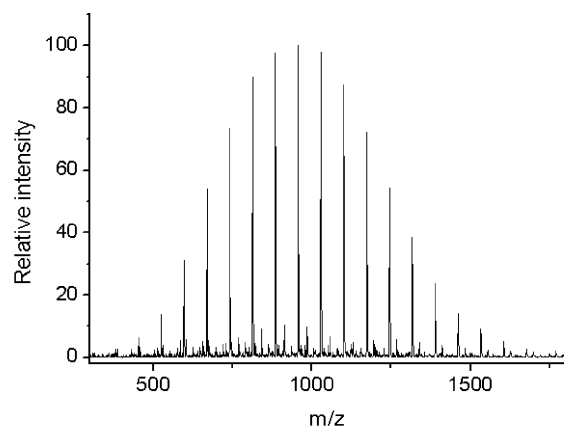


Figure 1. Electrospray mass spectroscopy (ESI-MS) distribution of polymeric species in a RAFT-acrylic acid polymerization in butanone. The target chain degree of polymerization in this example was 10 monomer units.

through an inhibitor removal column (Sigma Aldrich) twice to remove inhibitor and other artifacts. Granular NaOH (Sigma Aldrich) and the initiators 4,4'-azobis(4-cyanopentanoic acid) (V-501, Wako Industries) and potassium persulfate (KPS, Merck) were used as received. The RAFT agent, 2-[[butylsulfanyl]carbonothioyl]-sulfanyl]propanoic acid (denoted "RAFT V") was received in recrystallized form from Dulux Australia. *tert*-Butylhydroperoxide (TBHP, 70% aqueous solution, Sigma Aldrich), sodium hydrogen carbonate (Sigma Aldrich), butanone (Sigma Aldrich), and the surfactants AMA-80 (Cytec Industries) and sodium dodecyl sulfate (SDS, Sigma Aldrich) were used as received. All water used in this work was high-purity deionized water (Milli-Q).

Synthesis of Diblock Copolymers. The synthesis of a typical RAFTV-(AA)₅-(styrene)₅ was as follows:

RAFTV (1.49 g, 6.3 mmol) was dissolved in butanone (7.55 g). Deinhibited AA (2.29 g, 31.8 mmol) and V-501 (0.09 g, 0.3 mmol) were added to the reaction mixture and the solution stirred magnetically with high purity nitrogen bubbled through the mixture to remove any dissolved oxygen. The reaction vessel was heated to 70 °C and polymerization was allowed to take place for 2 h. A small drop of the reaction mixture was removed to check conversion by gravimetry (> 99% conversion) as well as the molecular weight distribution of the AA block via electrospray mass spectrometry (ESI-MS). All ESI-MS analysis was performed on a Finnigan Mat LCQ MS detector with Finnigan LCQ data processing and instrument control software. Polymeric samples were dissolved in a methanol/water 50:50 mixture, with a feed rate into the ionization unit of 0.2 mL min⁻¹. The applied voltage was 5 kV, with 7 kPa nitrogen acting as the aspirating gas. The heating element was at 200 °C. Figure 1 shows a sample ESI-MS spectrum of acrylic acid oligomers formed using this technique, indicating a narrow molecular weight distribution centered around the target average chain length (it is noted however that ESI-MS is not quantitative).

Further butanone (10 g) was added to the reaction mixture after cooling, with styrene (3.31 g, 31.7 mmol) and V-501 (0.09 g, 0.3 mmol) also added. After bubbling of nitrogen, polymerization was allowed to take place overnight at 70 °C. Conversion was checked by gravimetry.

Using an analogous procedure, RAFTV-(AA)₁₀-(styrene)₁₀ and RAFTV-(AA)₂₀-(styrene)₂₀ were synthesized using this technique.

Seed Latex Synthesis. A slightly modified technique to that described in Ferguson et al.¹³ was used in this work. Using the RAFTV-(AA)₅-(styrene)₅ diblock, the latex was made by the following procedure:

Diblock solution (6.09 g, containing 1.79 g of diblock) was dried in a vacuum oven overnight to remove butanone. Sodium hydroxide (0.39 g, 9.8 mmol) was dissolved in water (403 g), with the solution added to the vessel containing the dried diblock polymer. Equimolar amounts of sodium hydroxide and carboxylic acid groups were used to fully ionize the diblock polymer to assist dissolution.

V-501 (0.19 g, 0.6 mmol) was added to the solution and the mixture stirred magnetically while high-purity nitrogen was bubbled through the vessel. A temperature-controlled oil bath was preheated to 80 °C and the vessel lowered into it with continual stirring, after which a small amount of deoxygenated styrene (0.55 g, 5.2 mmol) was introduced to the vessel by syringe. Using an electronically controlled feed pump, styrene (46.05 g, 0.44 mol) was added to the mixture via gastight syringe using the following feed profile: 1.13 g/h for the first 2 h, followed by the remainder added at 10.58 g/h for the next 4 h. After all the styrene had been added, further V-501 (0.19 g dissolved in 9.04 g water) was added to the latex and the polymerization left overnight in order to polymerize any remaining monomer. The resultant latex was filtered through glass wool to remove any residual coagulum, and particle size measurements were checked by hydrodynamic chromatography (HDC) using a particle size distribution analyzer (Polymer Labs) and a capillary hydrodynamic fractionator (Matec). Average particle size and polydispersity results are quoted in Table 1. Particles formed by the RAFT-controlled self-assembly technique are of slightly higher polydispersity but significantly smaller size than those synthesized without RAFT.

Using the same procedure described above, latexes were synthesized using the (AA)₁₀ and (AA)₂₀ diblocks, with the three latexes referred to as ST5, ST10, and ST20, respectively. In all recipes the same relative amount of "surfactant" was used to keep the formulation as similar as possible between latex samples.

Removal/Modification of Active RAFT End Groups. Polymer chains in the latexes formed via the described method remain under RAFT control due to the presence of an active thiocarbonyl group on the end of each polymer chain within the interior of the particle, capable of undergoing reversible chain transfer. This will have a substantial effect on the overall polymerization kinetics, as has been seen through γ -relaxation experiments involving RAFT-mediated emulsion polymerization systems¹⁹ as well as Monte Carlo modeling,²⁰ where a significant increase in k is seen when a RAFT agent is present within the interior of a particle. As such, the RAFT end group must be chemically modified or destroyed in this system so that any effect on k that is seen is directly attributable to the hairy layer and not the RAFT agent. While various techniques to chemically modify RAFT end groups such as aminolysis,²¹ base-catalyzed hydrolysis²² and oxidation with peroxides and hydroperoxides²³ are successful in polymer solution, in this work it is crucial to retain the particle structure which is only possible under mild reaction conditions.

By modifying a similar technique described by Charmot et al.,²³ destruction of the thiocarbonyl group was achieved through the reaction with *tert*-butylhydroperoxide (TBHP). For every 50 g of latex, 1 g of TBHP was added with the latex heated at 80 °C for 24 h. TBHP proved to be water-soluble enough to transport through the aqueous phase and hydrophobic enough to enter a particle and react with the RAFT end groups. Discoloration of the latex from yellow to white was observed, indicating some chemical transformation had taken place, with virtually no coagulum at the conclusion of the reaction. To quantitatively determine the amount of RAFT agent removed, UV spectra of a polymer sample before and after the reaction were taken; the thiocarbonyl group is a chromophore.

UV spectra as a function of elution time of the polymer sample were recorded using size exclusion chromatography (SEC) with an on-line UV detector. This was performed on an Organic GPC (Shimadzu), consisting of in-line solvent degasser with a 0.1 μ m solvent filter, guard column (Waters) and a HR-2, HR-3, and HR-4 Styragel SEC columns (Waters) in series with one another. Columns were stored in a GPC column oven (Shimadzu) set at 30 °C. Samples were injected by an auto-injector (Shimadzu). First, 50 μ L of sample was injected into the column, with the mobile phase consisting of a 95:5 v/v % tetrahydrofuran/acetic acid (THF/AcA) mixture. Flow rate was set at 1 mL min⁻¹, with the signal response recorded by a RID-10A refractive index detector (Shimadzu). UV signal as a function of elution time was recorded on an SPD-10A-VP in-line UV detector, with the wavelength set at 290 nm. Figure

Table 1. Experimental Exit and Thermal Entry Rate Coefficients (Limit 2a) for Electrosterically Stabilized Latexes (Particle Size and Polydispersity Obtained from Polymer Labs HDC Equipment)

| latex type | av RAFT chains/particle | particle size (nm) (polydispersity) | average k (limit 2a) (s^{-1}) | expected k (limit 2a) (s^{-1}) | av ρ_{spont} (s^{-1}) |
|------------|-------------------------|--|--|---|---------------------------------------|
| ST0 | | 38.7 (1.01) | $(3.9 \pm 0.5) \times 10^{-2}$ | 1.7×10^{-2} | $(2.2 \pm 1.9) \times 10^{-5}$ |
| ST5 | 220 | 21.6 (1.07) | $(1.2 \pm 0.5) \times 10^{-2}$ | 4.3×10^{-2} | |
| ST10 | 232 | 21.4 (1.06) | $(5.0 \pm 1.2) \times 10^{-3}$ | 4.6×10^{-2} | |
| ST20 | 288 | 21.8 (1.08) | $(4.7 \pm 1.9) \times 10^{-3}$ | 4.4×10^{-2} | |

2 shows that there is essentially no change in the refractive index signal (indicating no significant modification of the molecular weight distribution of the polymer); however, the UV signal of the RAFT agent drops to almost zero, suggesting almost complete chemical modification. It has been reported²⁴ that the thiocarbonyl group is converted to a carbonyl group upon reaction with hydroperoxides, and it is likely that this has happened in this case.

Removal of Residual TBHP. TBHP is itself a chain-transfer agent (with a transfer constant of approximately 0.1 at 60 °C²⁵) due to a labile hydrogen atom, so it too must be removed from the latex, or otherwise the aqueous-phase chemistry would be affected. Being water-soluble, TBHP was removed by extensive dialysis of the latex (over several weeks) with twice-daily changes of water. To measure the amount of residual TBHP remaining, spectrophotometric measurements were taken by adding 1 mL of a 10% w/w solution of NaI in HCl to 1 mL of the aqueous phase of the latex. Any TBHP present will react with the iodide ion, with the evolution of iodine giving rise to a change in color that can be detected spectrophotometrically. After construction of a set of TBHP standards of varying concentrations, it was found that after 2 weeks dialysis the TBHP concentration was no more than 1.6 ppm. At this concentration the rate of chain transfer was assumed to be insignificant and was neglected with regard to further kinetic analysis.

Synthesis of Conventional Seed Latex. Sodium hydrogen carbonate (0.85 g, 10 mmol) and AMA-80 (8.48 g, 22 mmol) were added to water (405 g), and the resultant mixture was stirred magnetically to ensure complete dissolution. Deoxygenated styrene (49.8 g, 0.48 mol) was added to the reaction vessel and stirred vigorously to effect emulsification. High-purity nitrogen was bubbled through the emulsion to remove any dissolved oxygen for 30 min while the reaction vessel was brought to 90 °C. KPS (0.88 g, 3.2 mmol) dissolved in water (5 mL) was introduced via syringe, and polymerization took place for 5 h. The resultant latex was filtered through glass wool and dialyzed for 1 week to remove any residual surfactant. This latex (denoted ST0) was used as a benchmark to compare to our electrosterically stabilized particles.

Gamma Relaxation Dilatometry. For each seed latex, the following methodology was employed for seeded kinetic studies:

Styrene (5 g, 48 mmol), Milli-Q water (17 g), and seed latex (10 g) were separately degassed under vacuum and then loaded into a jacketed dilatometer vessel. SDS (0.005 g, 3.5 μmol) was added in order to stabilize monomer droplets, the dilatometer vessel sealed with a rubber septum, and the headspace evacuated via syringe at room temperature. Magnetic stirring of the solution took place overnight to allow transfer of monomer to the particle interior and the mixture then heated to 50 °C. Stirring was stopped, and the reaction vessel was evacuated again to remove dissolved oxygen.

A glass capillary (1.51 mm radius) was inserted into the top of the vessel, with water added until the solution was 10–12 cm up the capillary; stirring then recommenced. Dodecane (1 mL) was added to the top to prevent evaporation. Polymerization was initiated using a ⁶⁰Co γ source (dose rate = 105 Gy h⁻¹), available at the Australian Nuclear Science and Technology Organization (ANSTO). The automated dilatometer was lowered into the radiation source until the polymerization rate reached a steady state and then removed from the source, allowing the rate decrease to be monitored. The meniscus height was tracked automatically to provide conversion/time data. Multiple insertions and relaxations took place per sample in order to obtain a large number of experimental values.

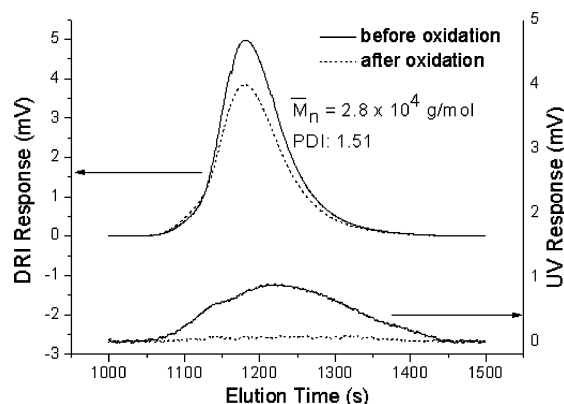


Figure 2. SEC trace (comprising refractive index and UV signals) as a function of elution time of poly(styrene-co-acrylic acid) before (solid line) and after (dotted line) the RAFT removal procedure. The UV signal is essentially zero after removal of the RAFT agent.

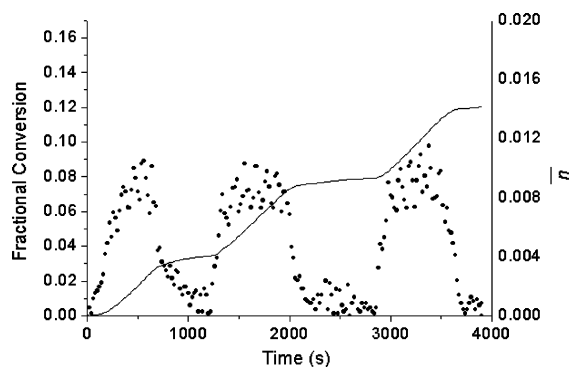


Figure 3. Typical conversion–time (solid line) and \bar{n} -time (dots) from a γ -relaxation experiment involving the ST5 latex. Multiple insertions were conducted per experiment to maximize the amount of experimental data.

Results and Discussion

Gamma Relaxation Experiments. A typical conversion–time plot from a γ -relaxation experiment involving multiple insertions into the radiation source is shown in Figure 3, with average rate coefficients for the four different latexes in question listed in Table 1. Extensive conversion/time data for all runs are given as Supplementary Information.

The first variation between the conventionally stabilized ST0 latex and the three electrosterically stabilized latexes in this study is that there was essentially no spontaneous (“thermal”) entry measured when electrosteric stabilization was present. It is well-known that there is a small, but measurable rate of polymerization in emulsion polymerizations in the absence of any added chemical initiator;²⁶ however, the origins of this polymerization are unclear. As spontaneously generated radicals from Diels–Alder dimerization reactions between styrene molecules are unlikely to form²⁷ at the relatively low temperature of 50 °C, the only likely source of spontaneously initiated polymerization is surface-generated peroxides formed during the seed latex synthesis.²⁶ While the spontaneous polymerization phenomenon is often dependent on latex preparation, it does seem striking

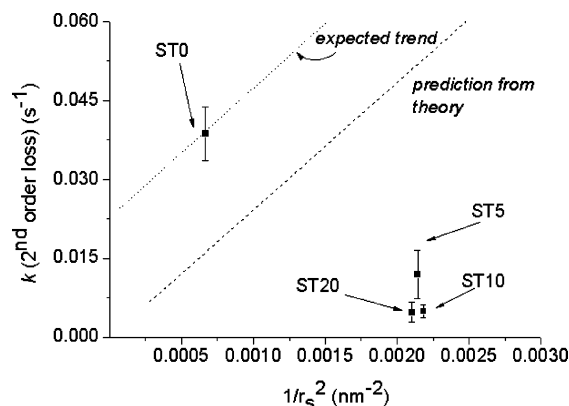


Figure 4. Normalized relaxation data (i.e., $\bar{n}/\bar{n}_{\text{initial}}$ so that the relaxation data begins at a value of 1 for all latexes) comparing ST0 (solid squares) and ST5 (open circles) latexes. Solid lines shown are the least-squares fit to eq 2, allowing k and ρ_{thermal} to be calculated.

that all three electrosterically stabilized latexes had no out-of-source polymerization rate in the relaxation experiments performed. This may be due to a number of reasons, one of which is that the presence of the polymeric layer grafted to the surface of the particle could prevent peroxides from forming on the surface or that any oxy-centered radicals generated react with the poly(AA) chains on the surface, restricting entry of thermally generated radicals. However, to have a more complete understanding of the thermal entry mechanism, specifically designed experiments involving radical traps²⁶ must be employed, which is not the focus of the current work.

The second and most important result from the γ -relaxation studies is that there is a significant variation in the exit rate coefficient k between electrostatically and electrosterically stabilized latexes. Even with an extremely short hairy layer (of average length 5 AA units), a substantial decrease in the exit rate coefficient is observed, as seen in the much longer relaxation time for the ST5 latex (Figure 4). The experimentally determined value of k decreases with increasing hydrophilic block length, although the values for ST10 and ST20 are almost identical. This decrease however is consistent with the postulate that the exit mechanism is restricted by the monomeric radical having to diffuse through a viscous polymeric layer on the surface of the particle. The fact that the k values for the three electrosterically stabilized latexes are substantially lower than that for ST0 also acts as another validation of the RAFT removal technique; it has been shown that for particles with RAFT concentrations as low as 1 mM that a 10-fold increase in the exit rate coefficient can occur,¹⁹ so the decrease in k observed in this work indicates that the removal of the active RAFT end groups was extremely successful.

One difficulty in comparing rate coefficients between latexes is that they are all of different average particle size (Figure 5). This is because while it is easy to grow small relatively monodisperse particle with poly(AA) stabilization using RAFT, there are currently no means to grow electrostatically stabilized latexes of the same small size with as low a size polydispersity. Now, k possesses an inverse square dependence on swollen particle radius.³ Thus, a means to take the particle size dependence into account is to divide the experimental k values by the limit 2a predicted k value for that particle size, this model having been shown to give excellent accord with experiment over a wide range of particle sizes with the results given in Table 2. One sees that the same trend is observed with both the exit rate coefficient ratio and the exit rate coefficient—a significant decrease from ST0 to ST5, with only a slight decrease

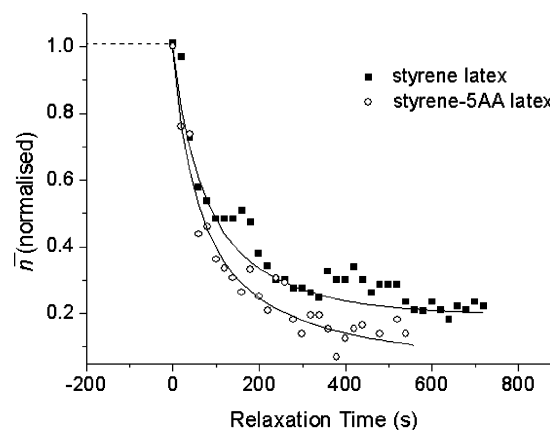


Figure 5. Experimental k values as a function of inverse square of the particle radius. Also shown are the predicted limit 2a k values from accepted theory (dashed line) as well as the expected trend (dotted line) from the ST0 latex.

Table 2. Ratio of Experimental Exit Rate Coefficient Value Compared to Theoretical Value as a Function of Size of Polymeric Layer

| latex type | $k_{\text{actual}}/k_{\text{theory}}$ |
|------------|---------------------------------------|
| ST0 | 2.3 ± 0.3 |
| ST5 | 0.28 ± 0.11 |
| ST10 | 0.11 ± 0.03 |
| ST20 | 0.11 ± 0.04 |

Table 3. Experimental and Theoretical Exit Rate Coefficients for Electrosterically Stabilized Latexes (Limit 1 kinetics)

| latex | experimental k (limit 1) (s^{-1}) | theoretical k (limit 1) (s^{-1}) | $k_{\text{exp}}/k_{\text{theory}}$ | theoretical ratio |
|-------|---|--|------------------------------------|----------------------|
| ST5 | $(6.8 \pm 1.6) \times 10^{-3}$ | 2.7×10^{-2} | 0.25 ± 0.06 | 0.38 |
| ST10 | $(5.1 \pm 1.7) \times 10^{-3}$ | 2.7×10^{-2} | 0.19 ± 0.06 | 0.31 |
| ST20 | $(5.1 \pm 1.4) \times 10^{-3}$ | 2.7×10^{-2} | 0.19 ± 0.05 | 0.24 |

thereafter when the average hydrophilic block length is extended up to 10 and 20 units. The decrease of a factor of 10 is very large and is indicative of the extent of the restriction of the exiting radical in electrosterically stabilized systems.

As the behavior of these electrosterically stabilized latexes is so different to what is predicted for electrosterically stabilized latexes of the same size, it is pertinent to consider the use of other kinetic limits in the processing of γ -relaxation data for calculating k . In zero-one systems, limit 1 kinetics is the case where complete termination of desorbed radicals in the aqueous phase occurs and there is no reentry event; as such, there is only a first-order dependence on \bar{n} . This is not likely in our systems because of the very low radical flux; however, there is the possibility that the reentry rate may conceivably also be slowed significantly, to the point where termination of these radicals in the aqueous phase might conceivably be their most likely fate (determining the impact that electrosteric stabilizers have on the entry mechanism is the subject of further work). Because of this uncertainty, the data are also processed using limit 1 kinetics.

The results for the calculated limit 1 k values are shown in Table 3 as well as the theoretically expected values for these latexes; for limit 1, the theoretical expression is given by

$$k = k_{\text{tr}}[M]_{\text{p}} \left(\frac{k_{\text{dM}}}{k_{\text{dM}} + k_{\text{p}}^1[M]_{\text{p}}} \right) \quad (5)$$

As seen in the limit 2a regime, the values of k obtained by treating the data with limit 1 kinetics are substantially lower than predicted by theory, with only a slow decrease at

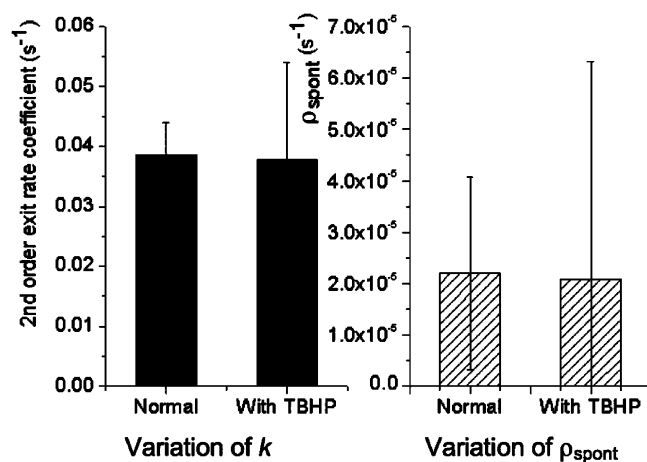


Figure 6. Comparison of experimental k and ρ_{spont} values for ST0 latex with no added TBHP (solid columns) vs that with 2 ppm TBHP (shaded columns).

longer hydrophilic block lengths. While the actual values themselves differ, the same qualitative trend can be seen from the data.

The Origin of the Observed Effect: Checking for Artifacts. While extreme care was taken to prevent impurities and other external factors influencing the observed results, there are two obvious possibilities for sources of experimental contamination: residual TBHP (a chain transfer agent) and RAFT oxidation byproducts, both of which could potentially alter the measured k values. To confirm that the reduced k values for the three electrosterically stabilized latexes was due to the “hairy layer” and not contaminants, two separate experiments were performed with ST0—an electrostatically stabilized latex. If any change in the behavior of this “normal” latex (i.e., without a hairy layer) was seen after contaminating the latex with either TBHP or RAFT oxidation byproducts, it could be claimed that the effect seen was not real.

First, a sample of ST0 was doped with a small amount of TBHP until a concentration of approximately 2 ppm was reached (the same concentration of hydroperoxide measured in the three electrosterically stabilized latexes after 2 weeks of dialysis following the oxidation reaction). The exit rate coefficient k and ρ_{spont} were measured for this latex using the γ -relaxation technique described previously, with multiple insertions into the radiation source to provide a set of experimental values. As seen in Figure 6, essentially the same values for k and ρ_{spont} were measured (within experimental error) for ST0 in the presence of 2 ppm TBHP, clearly indicating that residual TBHP is not the cause of the reduced k values in the three electrosterically stabilized systems. Significantly, the presence of TBHP (which is moderately water-soluble) did not lead to the absence of a spontaneous out-of-source polymerization rate.

To determine the significance of byproducts formed during the RAFT removal process, the “acetone transport” technique developed by Prescott et al.¹⁵ was utilized to transport the dodecyl analogue of the RAFT agent (used so that no RAFT agent will reside in the aqueous phase) into the interior of the particle. Then, 30 mg of the dodecyl RAFT agent was added to a 2:1 mixture of acetone:ST0 and was stirred at room temperature for 72 h with the organic cosolvent, allowing the transfer of the RAFT agent into the particle. The acetone was subsequently removed by a rotary evaporator (35 °C for 1 h), and the remaining latex was subjected to an identical RAFT removal treatment (2% w/w TBHP added with heating and stirring for 24 h at 80 °C) to that employed for the electrosteric latexes.

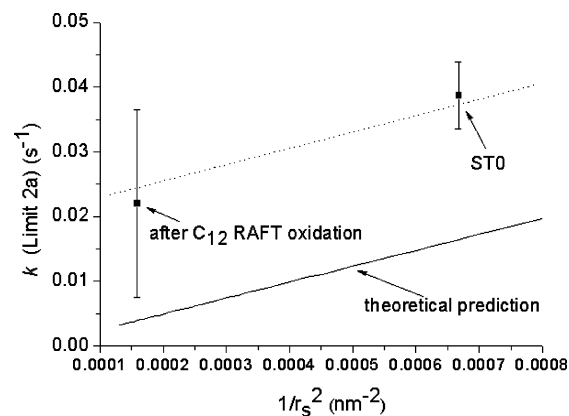


Figure 7. Experimental k values for ST0 latex before and after RAFT oxidation treatment as a function of $1/r_s^2$ (nm^{-2}). Also shown are theoretical values (solid line) and expected trend (dashes).

After 2 weeks of dialysis, both k and ρ_{spont} were measured via a series of γ -relaxation experiments.

In an unexpected result, the stability of ST0 to the RAFT removal procedure was questionable in comparison to the three electrosterically stabilized latexes studied. A significant increase in particle size (the swollen radius measured by HDC increased from 39.7 to 79.3 nm) was seen, most likely due to coalescence of particles under an extended period at elevated temperature in the absence of added surfactant. Not only does the value of the exit rate coefficient k vary with particle size³ making comparisons difficult, but the applicability of the appropriate kinetic limit is brought into question,²⁸ as the kinetic behavior may no longer be “zero–one”.

Assuming for the moment that limit 2a “zero–one” kinetics is still applicable for these larger latex particles, the obtained average experimental k value follows the expected $1/r_s^2$ proportionality relative to the untreated ST0 latex (Figure 7). Although the choice of kinetic limit is debatable in this case, the fact that while working within the same limit there is not a dramatic increase or decrease in k allows us to safely say that the observed experimental variation is due to the hairs on the particle surface and not to any byproducts formed during the RAFT removal. There was a clearly measurable “spontaneous” polymerization rate for this latex (with $\rho_{\text{spont}} \approx 10^{-4} \text{ s}^{-1}$), which also suggests that the absence of ρ_{spont} in the electrosteric latexes is due to the presence of the hairs on the surface.

Rationalization of Data and Mathematical Modeling. Both *ab initio*¹ and seeded^{10,11} kinetic studies on electrosterically stabilized latexes have suggested that diffusion through the polymeric layer on the surface has a significant impact on the interfacial mechanistic events that control the rate of an emulsion polymerization. While the importance of charge effects is well accepted when the polymeric hairs can be ionized and interact with a charged molecule, this work has shown that there is a significant restriction for an uncharged monomeric radical exiting a particle. This is in agreement with the modeling work of Asua,²⁹ whose calculations suggested that if the diffusion of an exiting species is slowed, the value of the exit rate coefficient can decrease significantly: a significant “steric” or diffusion effect imparted by the stabilizing layer.

The currently accepted model for exit is transfer of radical activity to monomer, followed by diffusion of the radical out into the aqueous phase with rate coefficient k_{dM} . For conventional emulsion systems, the mathematical modeling for k_{dM} is achieved by assuming the microscopic reversibility of the diffusion-controlled adsorption reaction (rate coefficient k_{ads}) onto a particle; it is assumed for these purposes that the diffusion

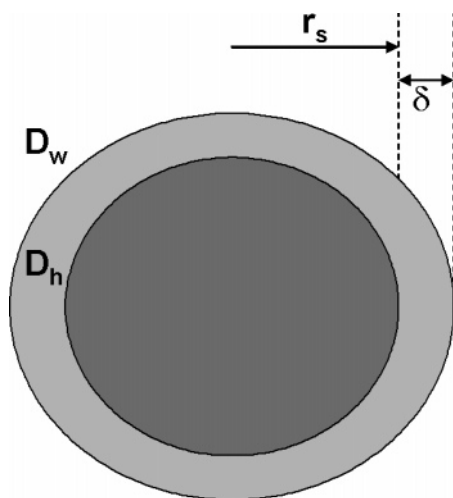


Figure 8. Model parameters for adsorption/desorption of a monomeric radical for electrosterically stabilized particles. Surrounding the particle of swollen radius r_s is a “hairy layer” of fixed width δ , with two separate diffusion coefficients: through the aqueous phase (D_w) as well as through the hairy layer (D_h).

coefficient and solubility of a monomeric radical in both water and particle phases are the same as that of a monomer molecule.³ (Note that this treatment is not in conflict with any assumption as to any subsequent reactions of the monomeric radical, such that it may enter another particle irreversibly; microscopic reversibility of adsorption and desorption is used solely to obtain the diffusion rates and solubilities of the radical, by assuming similarity to those of monomer.) For diffusion-controlled reactions such as this, the rate coefficient is given by the Smoluchowski equation, namely

$$k_{\text{ads}} = 4\pi D_w r_s N_{\text{Av}} \quad (6)$$

The reversibility of adsorption and desorption allows a mathematical description for k_{dM} , leading to eq 4.

For particles with electrosteric stabilization, a modified version of the Smoluchowski equation is required to account for the fact that the polymeric layer has a different diffusion coefficient to the aqueous phase; the following very simple treatment has similarities to the much more complex description derived by Asua.²⁹ A pictorial representation is given in Figure 8; a particle of swollen radius r_s with polymeric layer of fixed width δ , with differing diffusion coefficients for a monomeric species through both the aqueous phase (D_w) and the polymeric hairy layer (D_h). Assuming appropriate boundary conditions (with the derivation given in the Appendix), the expression for k_{ads} in this case is given by

$$k_{\text{ads}} = 4\pi \left(\frac{r_s(r_s + \delta)}{\delta + r_s(D_h/D_w)} \right) D_h N_{\text{Av}} \quad (7)$$

Assuming the reversibility of adsorption and desorption, we have a new expression for k_{dM} , namely

$$k_{\text{dM}} = 3D_h \frac{[M]_w}{[M]_p} \left(\frac{r_s + \delta}{r_s^2(\delta + r_s(D_h/D_w))} \right) \quad (8)$$

which is then used in the limit 2a expression for k . This of course reduces to eq 4 when $\delta = 0$.

Selection of Model Parameters. To compare this “restricted diffusion” model to experimental results, appropriate, realistic values for the parameters present in eq 8 must be determined.

Table 4. Parameters Values Used in “Restricted Exit” Model (see text for references)

| parameter | value |
|-----------------|--|
| D_w | $1.3 \times 10^{-9} \text{ m}^2 \text{ s}^{-1}$ |
| D_h | $2.4 \times 10^{-11} \text{ m}^2 \text{ s}^{-1}$ |
| $[M]_w$ | $4.3 \times 10^{-3} \text{ M}$ |
| $[M]_p$ | 6 M |
| k_{tr} | $9.3 \times 10^{-3} \text{ M}^{-1} \text{ s}^{-1}$ |
| k_p | $260 \text{ M}^{-1} \text{ s}^{-1}$ |
| k_p^1 | $4 k_p^1$ |
| δ (ST5) | 1.18 nm |
| δ (ST10) | 1.67 nm |
| δ (ST20) | 2.37 nm |

Values such as $[M]_w = 4.3 \times 10^{-3} \text{ M}$ (the saturation concentration of styrene in water at 50 °C) and $D_w = 1.3 \times 10^{-9} \text{ m}^2 \text{ s}^{-1}$ (the diffusion coefficient of a styrene monomer unit in water) are well accepted;⁵ estimation of δ and D_h are both nontrivial yet crucial to the accuracy of the exit model.

The estimation of δ (the width of the hairy layer) is complex. No reliable data exist for this property for such short chains, and theory (especially for a system such as this where the chain concentration is not in the dilute region) is not yet sufficiently reliable (see, e.g., the review by Dobrynin and Rubenstein³⁰). For the present, we make a number of assumptions to estimate this width. We first assume that every chain in the hairy layer is of identical length of 5, 10, or 20 units. This is not obviously not true given that a narrow distribution exists around the target average chain length from the RAFT polymerization technique and that chain burial within the particle can occur;¹³ however, it will serve as an effective approximation in this work. Using an appropriate chain extension factor (C_∞) for water-soluble polymer chains of 6.7¹² and assuming that the chain dimensions of tethered chains are 15–30% larger than free chains,³¹ the radius of gyration of the poly(AA) chains and hence the hairy layer width can be easily calculated. These chain lengths are reported in Table 4 (all benchmark values reported in Table 4 are quoted from Gilbert³).

The estimation of D_h (the diffusion coefficient of a styrene radical/monomer unit through the polymeric layer) is complicated, as no experimental data exist in this area, although diffusion coefficients of monomeric and oligomeric species in polymer solutions can be determined using pulsed-field gradient NMR (PFG NMR).³² The PFG NMR experiments of Strauch et al.³³ involve diffusion of a strongly hydrogen-bonded, water-soluble monomer, hydroxyethyl methacrylate (HEMA), in a water solution of its polymer. However, the diffusion coefficient values from this work are not entirely appropriate in our case, as the hydrophobicities of our monomer (styrene) and polymer (poly(AA)) are totally different, and this is likely to impact on the rate of diffusion.

The most applicable data in our case comes from the work of Yamane et al.³⁴ where spatial inhomogeneities in poly(AA) gels were detected by measuring the diffusion coefficient of probe molecules (poly(ethylene glycol) (PEG) standards) by PFG NMR. The lightly cross-linked gels in this work are of similar weight fraction polymer (w_p) (30%) to the surface coverage of our electrosterically stabilized latexes (approximately $40 \pm 10\%$ of the particle surface covered, calculated by surfactant titration). However, the average w_p value within the whole hairy layer is significantly lower than this “surface” value due to the presence of water around the hydrophilic polymer chains. The average w_p in the whole hairy layer was estimated as $\sim 5\%$ for all three latexes, found by calculating the mass of poly(acrylic acid) on each particle surface (i.e., the number (moles) of AA units per chain multiplied by the average number

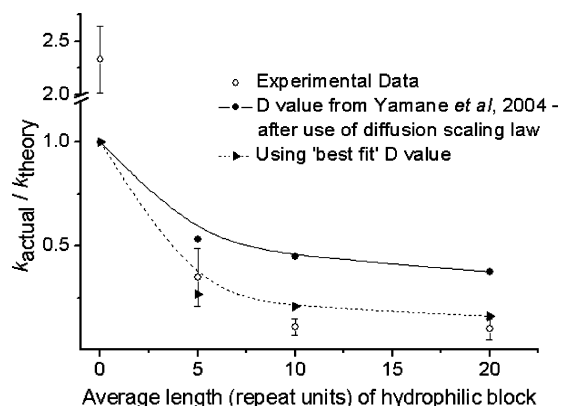


Figure 9. Comparison of experimental k ratio data (open circles) with new diffusion model (filled circles (using diffusion coefficients from Yamane et al.³⁴) and filled triangles (“best fit” diffusion coefficient value)).

of chains per particle (Table 1), converted into mass) as well as the volume of the hairy layer shell around the particle. Explicitly:

$$w_p = \frac{\bar{X}_n(\text{AA})n_{\text{chains}}\frac{m_{\text{AA}}}{N_{\text{Av}}}}{\frac{4}{3}\pi((r_s + \delta)^3 - r_s^3)d_{\text{water}}} \quad (9)$$

where $\bar{X}_n(\text{AA})$ = number-average degree of polymerization of the AA units per chain, n_{chains} = number of chains per particle, m_{AA} = molar mass of acrylic acid, and d_{water} = density of water.

Yamane et al.³⁴ found, for only slightly swollen gels, two diffusion coefficients as a function of pulse interval time. Here the lower value was used as set out below to estimate D_h , as this represents short-range diffusion through small distances, which is more applicable considering the dimensions of the hairy layer on the particle surface.

Using these conditions, a value of $D = 4.4 \times 10^{-13} \text{ m}^2 \text{ s}^{-1}$ was reported³⁴ for the PEG probe molecule, which was a short chain polymer with $M_n = 1500$. The corresponding degree of polymerization is 25, and this species will diffuse far slower than a monomeric unit. Using the well-tested empirical diffusion scaling law,³⁵ namely

$$D_i = \frac{D_{\text{mon}}}{i^{0.66+2w_p}} \quad (10)$$

where i is the degree of polymerization of the oligomer in question. This then yields a value of $D_{\text{mon}} = 2.5 \times 10^{-11} \text{ m}^2 \text{ s}^{-1}$, approximately 50 times lower than D_w . This is the value applicable at the w_p of Yamane et al.,³⁴ viz., 0.3. This then must be converted to a value applicable for the w_p estimated for the hairy layer, viz., 0.05. For this purpose, we scale the diffusion coefficient by the ratio of diffusion coefficients predicted for the same values of w_p using the free-volume fitting of HEMA diffusion data by Strauch et al.³³ which yields $D_{\text{mon}} = 7.3 \times 10^{-11} \text{ m}^2 \text{ s}^{-1}$. Using this value of D_{mon} to represent D_h in our model, the comparison between the model and our experimental data points given in Figure 9 shows that the observed trend with $\bar{X}_n(\text{AA})$ is reproduced acceptably, but not the absolute values. Given the many uncertainties involved in this estimation of D_h , it was deemed acceptable to adjust its value somewhat, and it was found (see Figure 9) that decreasing this by a factor of 3 (which we feel is reasonable) gives good absolute agreement with the data. Using the same value of D_h , Limit 1 k values can

also be predicted via this model, shown in Table 3. Once again the same excellent agreement between experiment and theory is seen, and while the actual fate of exited radicals (i.e., whether the system obeys limit 1 or limit 2a) cannot yet be elucidated, the same effect on both approaches is seen.

Taking into consideration that there is significant uncertainty in estimating D_h , it is felt that the mathematical model developed in this work is able to rationalize and semiquantitatively predict exit rate coefficient values for electrosterically stabilized latex particles. Quantitative prediction must await better experimental data and theory for both the spatial extent (and inhomogeneity therein) of the hairy layer, and of diffusion coefficients of appropriate species in this semidilute aqueous polymer solution.

The data above suggest that, even for a monomeric species, diffusion through a polymeric “hairy layer” is strongly restricted, and a major influence on exit kinetics is seen as a result. It is expected that the same significant impact of a hairy layer will be seen in the entry rate coefficient for analogous systems, with the added effect of charge interactions when ionic initiators are used.

Comparison with Other Established Models. A first-principles model for radical desorption kinetics was recently developed by Asua²⁹ that also incorporates the effect due to the presence of a layer of steric surfactant on the surface of the particle. Similar to the model presented in this work, the model presented by Asua requires parameters such as the width of the hairy layer and the diffusion coefficient of the desorbed monomeric radical through this layer, and thus comparison between the two models is of high interest. Now, Asua’s treatment yields an expression for the rate coefficient for radical desorption, and being very general, should be applicable to zero–one conditions such as are deliberately chosen here. Our use of a zero–one system enables such a rate coefficient to be related to the experimental observable, viz., the rate of radical loss, with a minimum of model-based assumptions. While it is impossible to refute or support proposed mechanisms using Asua’s very general approach, as there are more adjustable parameters than unambiguous pieces of experimental data (unlike the use of the simple kinetic limits, zero–one in the present case, that can be fitted to experiment), it is nonetheless an interesting exercise to compare the two approaches.

The rate coefficient expression for radical desorption presented by Asua is

$$k = \lambda \frac{\gamma N_{\text{Av}}}{\eta m} \left(1 - \frac{\lambda N_p}{\lambda N_p + k_p[M]_w + 2k_t[R]_w} \right) \quad (11)$$

where

$$\eta = \frac{k_p[M]_p}{D_p} \quad (12)$$

$$\gamma = \frac{\left(\frac{k_t[M]_p}{V_s N_{\text{Av}}} \right)}{D_p} \quad (13)$$

$$\lambda = \frac{4\pi D_w r_s}{1 + \frac{D_w}{D_h} \frac{\delta}{r_s} + \frac{D_w}{D_p m} \frac{1}{r_s \sqrt{\eta} \coth(r_s \sqrt{\eta}) - 1}} \quad (14)$$

where D_p is the diffusion coefficient of a monomeric radical inside a latex particle, V_s the swollen volume of a latex particle, k_t the bimolecular termination rate coefficient in the aqueous

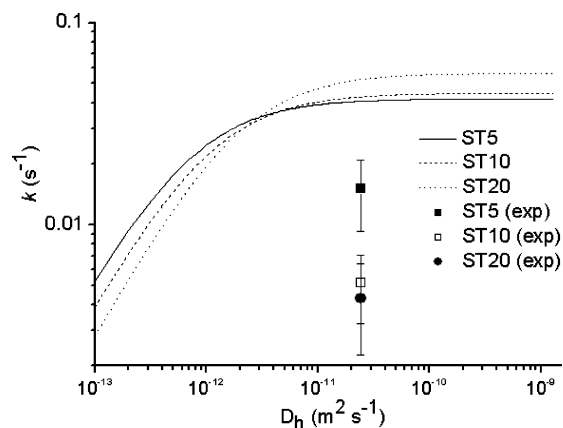


Figure 10. Experimental k values for electrosterically stabilized latexes with comparison to theoretical desorption model developed by Asua.²⁹ Key: Solid line, filled square = ST5 ($N_p = 3.22 \times 10^{18} \text{ L}^{-1}$); dashed line and open square = ST10 ($N_p = 3.2 \times 10^{18} \text{ L}^{-1}$); dotted line and filled circle = ST20 ($N_p = 2.4 \times 10^{18} \text{ L}^{-1}$).

phase, $[R]_w$ the concentration of radicals in the aqueous phase, and m the partition coefficient relating the concentration of monomeric radicals at either side of the particle/hairy layer interface.²⁹ All other parameters are the same as identified previously.

As pointed out by a number of authors (e.g., Gilbert et al.^{3,36} and Asua²⁹), the definition of an exit (or desorption) rate coefficient is often ambiguous, because this definition depends on the fate of exited free radicals (especially in the aqueous phase), and whether the definition counts as “true” exit an exited monomeric radical which reenters another particle and continues polymerization without loss of radical activity. The great advantages of treating emulsion polymerization kinetics as two limiting cases (zero—one and pseudo-bulk, and the subdivision of the former into various limits, limit 1 and limit 2a being discussed here) are (a) that this definition is then quite unambiguous, and (b) that the exit rate coefficient can be obtained uniquely from experiment without any model assumptions except as to which limit is involved (the applicable limit in turn can usually be deduced from simple order-of-magnitude estimates of various rate coefficients,^{5,28} although in the present case that must await further data on the effect of a hairy layer on radical entry). This is a different philosophical approach from that of Asua, who gives a very detailed quantitative mechanistic description for radical exit which incorporates all zero—one cases (although not the general pseudo-bulk limit, because chain-length dependent termination is not included). While optimal for modeling purposes, Asua’s description does not permit unambiguous comparison between model and experiment, because the model contains many parameters whose values are hard to determine with sufficient precision.

Asua’s model predicts a significant decrease in k is seen when D_h is decreased, all other parameters being constant, which is consistent with the experimental trend seen in this work (as a densely covered particle surface restricts the diffusion of the monomeric radical). Because, as just stated, it is impossible to make an unambiguous direct comparison of Asua’s model with experiment without choosing values of rate parameters which cannot be accurately determined independently, we carry out this comparison by choosing what we feel are the best available values.

Using the parameters quoted in Table 4 as well as $D_p = 2 \times 10^{-10} \text{ m}^2 \text{ s}^{-1}$,²⁹ $m = 70$,²⁹ and $k_t = 1.75 \times 10^9 \text{ M}^{-1} \text{ s}^{-1}$,²⁸ the variation of k from eq 11 as a function of D_h is shown in Figure 10 for the three electrosterically stabilized latexes in question.

In choosing the various parameter values, a value of $[R]_w = 3 \times 10^{-9} \text{ M}$ was chosen so that the k values from eqs 2 and 11 were in agreement for latexes of this size with no hairy layer; it is noted that $[R]_w$ will vary with each system and indeed with the time evolution of the radiolysis system as it is removed from the source, but decreasing this quantity by an order of magnitude only changes the calculated value of k by 30%. As expected, there is a slight calculated decrease in k as the width of the hairy layer is increased (although this decrease does not hold for all values of D_h due to the slightly different N_p values). The experimentally determined k values for ST5, ST10 and ST20 are also shown in Figure 10 at the “best” value for D_h used in the modeling work discussed earlier ($D_h = 2.42 \times 10^{-11} \text{ m}^2 \text{ s}^{-1}$). The experimental values show the same decrease in k as the width of the hairy layer increases; however the k values are far lower than predicted by Asua’s model. The reason for the discrepancy cannot be ascertained at present, because as stated the model contains parameters whose values have not been determined independently. One means of comparison would be to analyze latexes with different surface coverages (and hence different D_h values) to see the predictive behavior of both models.

Conclusions

Electrosterically stabilized latexes with differing lengths of poly(AA) stabilizing blocks were synthesized by the “RAFT-in-emulsion” technique in order to study the exit kinetics of styrene in such systems. Having model latexes with controlled hairs grafted to the surface has allowed, for the first time, the behavior of the exit rate coefficient k to be studied as a function of polymer chain length.

Using γ -relaxation experiments, k as well as the thermal entry rate coefficient were determined for three electrosterically stabilized latexes (with poly(AA) blocks of length 5, 10, and 20 grafted to the surface) as well as an electrostatically stabilized latex for comparative purposes. The methodology of choosing conditions so that zero—one kinetics were obeyed meant that the exit rate coefficient can be unambiguously defined in terms of, and unambiguously determined from, the experimental data, which comprise the variation in rate as the polymerization system is suddenly removed from the source of initiating radicals.

It was shown that even short “hairs” led to a substantial decrease in the exit rate coefficient relative to an ionically stabilized system, with k decreasing as a function of hairy layer width. This decrease was quantitatively indicative of a diffusion-controlled process whereby the exiting monomeric radical is strongly restricted from exiting a particle. The value of the “spontaneous” entry rate coefficient was found to be negligible for these electrosterically stabilized systems, which may be attributable to “spontaneously” formed radicals (perhaps from peroxides formed during the seed latex preparation process) being trapped by or reacting with the poly(AA) hairs on the surface of the particle.

Through a modification of the Smoluchowski equation for diffusion-controlled reactions in solution (with some of the same starting points as the more general treatment of Asua²⁹), a quantitative description for the rate coefficient for desorption (k_{dM}) of a monomeric radical in this system was deduced, giving the quantitative dependences of the loss rate coefficient on both the width of the hairy layer and the diffusion coefficient of a radical within the hairy layer. On the basis of estimates from data where diffusion coefficients of probe molecules within lightly cross-linked poly(AA) gels were measured, the diffusion

coefficient of a monomeric radical within our polymeric layer was estimated to be approximately 50 times lower than in water. This value gave semiquantitative agreement with experimentally obtained values, and a good reproduction of the observed trend with the degree of polymerization in the hairs, validating the postulate that restricted exit through a lower diffusion coefficient is the controlling mechanism for exit in these systems.

As radical exit is only one of the two dominant mechanistic processes in styrene emulsion polymerization involving small particles, future work in this area will turn to radical entry in electrosterically stabilized systems.

Acknowledgment. The financial support of a Discovery Grant from the Australian Research Council and an Australian Postgraduate Award (APA) are gratefully acknowledged, as is a grant provided by the Australian Institute of Nuclear Science and Engineering (AINSE). Dr. Dimitri Alexiev and Mr. David Sangster are thanked for their help and input with regards to the use of γ -radiation facilities for dilatometric experiments, and Dr. Kim van Berkel for insightful comments on the gamma dilatometry data. Ms Hollie Zondanos is gratefully acknowledged for conducting the mass spectrometry measurements. The Key Centre For Polymer Colloids was established and supported by the Australian Research Council's Research Centres Program.

Appendix

By modifying the Smoluchowski equation for a radical adsorbing onto the particle by including diffusion through both the aqueous phase and then a hairy layer of fixed width, a mathematical expression for k_{dM} (the rate coefficient for radical desorption) can be found.

Fick's 2nd law states

$$\frac{\partial c}{\partial t} = D \nabla^2 c \quad (\text{A.1})$$

where D is the diffusion coefficient of the medium and c is the concentration of radicals. There are two regions of interest—inside the hairy layer (c_h) and in the aqueous phase (c_w). Assuming steady-state conditions for both regions, the problem reduces to solving $\nabla^2 c = 0$.

Assuming spherically symmetric coordinates, we obtain the second order differential equation

$$\frac{d^2 c}{dr^2} + \frac{2}{r} \frac{dc}{dr} = 0 \quad (\text{A.2})$$

where r is the radial displacement from the origin of the system (the center of the spherical particle). Using a simple reduction-of-order method the general solution of these equations is

$$c = a + \frac{b}{r} \quad (\text{A.3})$$

where a and b are constants. Let us assume that this equation holds in both regions, with the constants a and b controlled by the boundary conditions in this system. The swollen radius of the particle is r_s , and the width of the hairy layer is δ . For an interface-boundary problem, at the interface of the water and the hairy layer, the concentration of the radicals must be continuous (approach the same limit from either side of the interface) and the flux across this surface must be identical for both equations, i.e.

$$-D_h \left. \frac{dc_h}{dr} \right|_{r=r_s+\delta} = -D_w \left. \frac{dc_w}{dr} \right|_{r=r_s+\delta} \quad (\text{A.4})$$

These restrictions dictate what values the constants will take. Let

$$c_h = a_h + \frac{b_h}{r} \quad (\text{A.5})$$

When $r = r_s$, $c_h = 0$. Therefore

$$a_h = -\frac{b_h}{r_s} \quad (\text{A.6})$$

and

$$c_h = b_h \left(\frac{1}{r} - \frac{1}{r_s} \right) \quad (\text{A.7})$$

When $r = \infty$, $c_w = c_{\text{inf}}$ (to be defined later). Hence

$$a_w = c_{\text{inf}} \quad (\text{A.8})$$

and

$$c_w = c_{\text{inf}} + \frac{b_w}{r} \quad (\text{A.9})$$

Using the conditions mentioned above, when $r = r_s + \delta$, $c_w = c_h$. Therefore

$$c_{\text{inf}} + \frac{b_w}{r_s + \delta} = -b_h \left(\frac{\delta}{r_s(r_s + \delta)} \right) \quad (\text{A.10})$$

Similarly the condition from the requirement that the radical fluxes must be equivalent yields

$$D_w \left(\frac{b_w}{(r_s + \delta)^2} \right) = D_h \left(\frac{b_h}{(r_s + \delta)_2} \right) \quad (\text{A.11})$$

or simply $D_w b_w = D_h b_h$. Rearranging eq A.11 we have

$$b_w = \frac{D_h}{D_w} b_h \quad (\text{A.12})$$

and so

$$c_{\text{inf}} + \frac{D_h}{D_w} \frac{b_h}{(r_s + \delta)} = -b_h \left(\frac{\delta}{r_s(r_s + \delta)} \right) \quad (\text{A.13})$$

which upon rearrangement gives us the expression

$$b_h = -c_{\text{inf}} \left(\frac{r_s(r_s + \delta)}{\delta + r_s(D_h/D_w)} \right) \quad (\text{A.14})$$

Therefore, the concentration of monomeric radicals inside the hairy layer is

$$c_h = c_{\text{inf}} \left(\frac{r_s(r_s + \delta)}{\delta + r_s(D_h/D_w)} \right) \left(\frac{1}{r_s} - \frac{1}{r} \right) \quad (\text{A.15})$$

The flux at the surface of the particle is therefore

$$-D_h \left. \frac{dc_h}{dr} \right|_{r=r_s} = -D_h \frac{b_h}{r_s^2} \quad (\text{A.16})$$

and so the rate of reaction at the surface is equal to

$$4\pi r_s^2 \times (\text{radical flux}) = 4\pi c_{\text{inf}} \left(\frac{r_s(r_s + \delta)}{\delta + r_s(D_h/D_w)} \right) D_h \quad (\text{A.17})$$

As the rate of entry can also be written as $k_{\text{ads}}[M](N_p/N_{\text{Av}}) = k_{\text{ads}}[M][P]$, where $[P]$ is the concentration of particles, then the number of particles $P = N_{\text{Av}}[P]V$ where V is the volume of the system.

Hence the global flow of radicals equals

$$4\pi c_{\text{inf}} \left(\frac{r_s(r_s + \delta)}{\delta + r_s(D_h/D_w)} \right) D_h N_{\text{Av}} [P] V \quad (\text{A.18})$$

Rearranging eq A.18 gives the “modified” expression for k_{ads} :

$$k_{\text{ads}} = 4\pi \left(\frac{r_s(r_s + \delta)}{\delta + r_s(D_h/D_w)} \right) D_h N_{\text{Av}} \quad (\text{A.19})$$

From this expression and the principle of microscopic reversibility, we can formulate an expression for the desorption of a monomeric radical (M^\bullet) in this system.



The rate of monomer molecules being captured by a given particle is $k_{\text{ads}}[M]_w$, while the total rate of escaping per unit time is given by $k_{\text{dM}}V_s[M]_pN_{\text{Av}}$. Equating these two (when at equilibrium) gives allows us to rearrange and solve for k_{dM} , namely:

$$k_{\text{dM}} = 3D_h \frac{[M]_w}{[M]_p} \left(\frac{r_s + \delta}{r_s^2(\delta + r_s(D_h/D_w))} \right) \quad (\text{A.21})$$

Supporting Information Available: Figures S1–S4, showing several sets of conversion–time data from γ -radiolysis experiments performed on different emulsion polymerization systems. This material is available free of charge via the Internet at <http://pubs.acs.org>.

References and Notes

- (1) Leemans, L.; Jerome, R.; Teyssie, P. *Macromolecules* **1998**, *31*, 5565–5571.
- (2) Smith, W. V.; Ewart, R. H. *J. Chem. Phys.* **1948**, *16*, 592–599.
- (3) Gilbert, R. G. *Emulsion Polymerisation: A Mechanistic Approach*; Academic Press: San Diego, CA, 1995.
- (4) Hawket, B. S.; Napper, D. H.; Gilbert, R. G. *J. Chem. Soc., Faraday Trans. 1* **1980**, *76*, 1323–1343.
- (5) Casey, B. S.; Morrison, B. R.; Maxwell, I. A.; Gilbert, R. G.; Napper, D. H. *J. Polym. Sci., Part A: Polym. Chem.* **1994**, *32*, 605–630.
- (6) Nomura, M. In *Emulsion Polymerization*; Piirma, I., Ed.; Academic: New York, 1982; pp 191–219.
- (7) Ugelstad, J.; Hansen, F. K. *Rubber Chem. Technol.* **1976**, *49*, 536–609.
- (8) van Berkel, K. Y.; Russell, G. T.; Gilbert, R. G. *Macromolecules* **2003**, *36*, 3921–3931.
- (9) Maxwell, I. A.; Morrison, B. R.; Napper, D. H.; Gilbert, R. G. *Macromolecules* **1991**, *24*, 1629–1640.
- (10) Vorwerg, L.; Gilbert, R. G. *Macromolecules* **2000**, *33*, 6693–6703.
- (11) Coen, E. M.; Lyons, R. A.; Gilbert, R. G. *Macromolecules* **1996**, *29*, 5128–5135.
- (12) De Bruyn, H.; Gilbert, R. G.; White, J. W.; Schulz, J. C. *Polymer* **2003**, *44*, 4411–4420.
- (13) Ferguson, C. J.; Hughes, R. J.; Nguyen, D.; Pham, B. T. T.; Gilbert, R. G.; Serelis, A. K.; Such, C. H.; Hawket, B. S. *Macromolecules* **2005**, *38*, 2191–2204.
- (14) Chiefari, J.; Chong, Y. K.; Ercole, F.; Krstina, J.; Jeffery, J.; Le, T. P. T.; Mayadunne, R. T. A.; Meijs, G. F.; Moad, C. L.; Moad, G.; Rizzardo, E.; Thang, S. H. *Macromolecules* **1998**, *31*, 5559–5562.
- (15) Prescott, S. W.; Ballard, M. J.; Rizzardo, E.; Gilbert, R. G. *Macromolecules* **2002**, *35*, 5417–5425.
- (16) Adams, M. E.; Trau, M.; Gilbert, R. G.; Napper, D. H.; Sangster, D. F. *Aust. J. Chem.* **1988**, *41*, 1799–1813.
- (17) Gilbert, R. G.; Napper, D. H. *J. Macromol. Sci.—Rev. Macromol. Chem. Phys. C* **1983**, *23*, 127–186.
- (18) Maxwell, I. A.; Sudol, E. D.; Napper, D. H.; Gilbert, R. G. *J. Chem. Soc., Faraday Trans. 1* **1988**, *84*, 3107–3112.
- (19) Prescott, S. W.; Ballard, M. J.; Rizzardo, E.; Gilbert, R. G. *Macromolecules* **2005**, *38*, 4901–4912.
- (20) Prescott, S. W. *Macromolecules* **2003**, *36*, 9608–9621.
- (21) Wang, Z.; He, J.; Tao, Y.; Yang, L.; Jiang, H.; Yang, Y. *Macromolecules* **2003**, *36*, 7446–7452.
- (22) Schilli, C.; Lanzendoerfer, M. G.; Mueller, A. H. E. *Macromolecules* **2002**, *35*, 6819–6827.
- (23) Charnot, D.; Chang, H. T.; Wang, W.; Piotti, M. Symyx Technologies, Inc.: 2003; U.S. Patent Appl. 963,172.
- (24) Vana, P.; Albertin, L.; Barner, L.; Davis, T. P.; Barner-Kowollik, C. *J. Polym. Sci., Part A: Polym. Chem.* **2002**, *40*, 4032–4037.
- (25) Odian, G. *Principles of Polymerization*, 4th ed.; Wiley-Interscience: New York, 2004.
- (26) Christie, D. I.; Gilbert, R. G.; Congalidis, J. P.; Richards, J. R.; McMinn, J. H. *Macromolecules* **2001**, *34*, 5158–5168.
- (27) Olaj, O. F.; Kauffmann, H. F.; Breitenbach, J. W. *Makromol. Chem.* **1977**, *178*, 2707–2717.
- (28) Morrison, B. R.; Casey, B. S.; Lacik, I.; Leslie, G. L.; Sangster, D. F.; Gilbert, R. G.; Napper, D. H. *J. Polym. Sci., Part A: Polym. Chem.* **1994**, *32*, 631–649.
- (29) Asua, J. M. *Macromolecules* **2003**, *36*, 6245–6251.
- (30) Dobrynin, A. V.; Rubinstein, M. *Prog. Polym. Sci.* **2005**, *30*, 1049–1118.
- (31) Feigin, R. I.; Napper, D. H. *Colloid Polym. Sci.* **1980**, *258*, 1153–1158.
- (32) Callaghan, P. T. *Austr. J. Phys.* **1984**, *37*, 359–387.
- (33) Strauch, J.; McDonald, J.; Chapman, B. E.; Kuchel, P. W.; Hawket, B. S.; Roberts, G. E.; Tonge, M. P.; Gilbert, R. G. *J. Polym. Sci., Part A: Polym. Chem.* **2003**, *41*, 2491–2501.
- (34) Yamane, Y.; Ando, I.; Buchholz, F. L.; Reinhardt, A. R.; Schlick, S. *Macromolecules* **2004**, *37*, 9841–9849.
- (35) Griffiths, M. C.; Strauch, J.; Monteiro, M. J.; Gilbert, R. G. *Macromolecules* **1998**, *31*, 7835–7844.
- (36) Whang, B. C. Y.; Napper, D. H.; Ballard, M. J.; Gilbert, R. G.; Licht, G. *J. Chem. Soc., Faraday Trans. 1* **1982**, *78*, 1117.

MA052224D